*The 2010 STScI Calibration Workshop*
*Space Telescope Science Institute, 2010*
*Susana Deustua and Cristina Oliveira, eds.*

# Multi – Wavelength Geometric Distortion Solution for WFC3/UVIS and IR

V. Kozhurina-Platais[1], C. R. Cox[1], L. Petro[1], M. Dulude[1], J. Mack[1]

*Space Telescope Science Institute, Baltimore, MD, 21218*

**Abstract.** The standard astrometric catalog based on ACS/WFC observations of the globular cluster $\omega$ Cen field has been used to examine the geometric distortion of WFC3/UVIS and IR as a function of wavelength. Multiple observations of this field taken with large dither patterns and a large range of the HST roll-angles were exposed through 10 UVIS and 5 IR band-passes. A 4th order polynomial model was used to derive the geometric distortion coefficients relative to the distortion free coordinates of our astrometric field in the UVIS and IR channels. The main results of this calibrations are: 1) geometric distortion can be successfully corrected at the 0.1 pixels (4 and 10 *mas*) precision level in UVIS and IR channels, respectively; 2) the non-perpendicularity of coordinate axes (skew) can be used to assess the scale change from filter to filter, time, and HST roll-angle; 3) the coefficients of the geometric distortion in the UVIS and IR channels are used in STScI Multidrizzle software in order to correct WFC3 images for distortion.

## 1. Introduction

A new instrument, *Wide Field Camera 3* (WFC3), a fourth generation imaging instrument of *HST*, was installed on *HST* during Servicing Mission 4 in May 2009. The Servicing Mission Orbital Verification (SMOV) observations (proposal 11444, and 11445, PI–L. Dressel) with the WFC3/UVIS and IR channels were used to derive the geometric distortion only for one filter, F606W and F160W, in UVIS and IR, respectively. A preliminary optical ray-tracing model demonstrated that the geometric distortion in WFC3/UVIS and IR cameras is severe, on the order of $\sim 7\%$ across the detector. This distortion in the form of displacement of celestial sources from their true positions on the sky can reach up to about 120 pixels or $\sim 5''$ in UVIS and 35 pixels, or $\sim 4''$ in IR. The knowledge of accurate geometric distortion is important not only for deriving accurate positions, parallaxes and proper motions of the scientifically interesting objects but also to rectify the WFC3 images. The Multidrizzle software (Koekemoer 2002, ), currently installed in the STScI on-the-fly pipeline (OTFR), requires accurate distortion correction in order to combine dithered WFC3 images (UVIS and IR), to enhance spatial resolution, and to deepen the detection limit. If the geometric distortion correction implemented in Multidrizzle is not accurate enough, then the WFC3 combined frames can produce blurred images and distort the under-sampled Point Spread Function (PSF). Any significant uncertainty in the geometric distortion correction is detrimental to alignment of WFC3 images with MultiDrizzle and to mitigating the effect of an under-sampled PSF.

The goal of this multi-wavelength astrometric calibration was to derive an accurate geometric distortion in 10 UVIS and 5 IR filters to a precision level of 0.1 pixels (or 4 and 10 *mas* respectively), which is sufficient to combine dithered and mosaic *WFC3* UVIS and IR images using the STSDAS Multidrizzle software.

Here, we present the analysis and results of geometry distortion calibration, now sufficiently accurate to use in Multidrizzle with observations of the new *HST* camera *WFC3* in UVIS and IR chanells.

## 2. Observations and Reductions

The standard astrometric catalog in the vicinity of globular cluster $\omega$ Cen was used for a multi-wavelength geometric distortion calibration of UVIS and IR. The tangent–plane projection type positions (further referred to as the $U, V$ rectangular coordinate system) of stars in the standard astrometric catalog are globally accurate to $\sim$0.02 ACS/WFC pixels or 1*mas* (Anderson & van der Marel, 2010). The globular cluster $\omega$ Cen was observed with UVIS and IR detectors near the center of the standard astrometric catalog with large dither patterns and at different HST roll-angles (CAL–11911, PI–E. Sabbi and CAL–11928, PI–V. Kozhurina-Platais). The observations were taken through 10 UVIS filters and 5 IR filters. The supplemental calibration program (CAL–12094, PI–L.Petro) also observed $\omega$ Cen with UVIS through F606W filter at different HST roll-angles from –95° to –135° at a step of –10°.

The reductions and analysis of multi-wavelength geometric distortion for UVIS and IR observations are similar to the reductions used in the SMOV UVIS and IR geometric distortion calibration and described in detail by Kozhurina-Platais *et al.*, (2009a, 2009b). At the time of our analysis, there were no high precision tools available such as an *effectivePSF* library as has been derived for the ACS/WFC camera (Anderson, 2002). Therefore, IRAF task – DAOPHOT/PHOT, which includes a Gaussian fit to the PSF centroid and simultaneous aperture photometry was used to obtain the $X$ & $Y$ positions of stars on each of the UVIS CCD chips for a total of 200 UVIS images. Nevertheless, the IR *ePSF* library was available (Anderson, 2010) at the time of IR analysis, Thus, the *ePSF* fitting technique was used to obtain an accurate and high-precision $X$ & $Y$ positions of stars on each of the IR images for total of 90 IR images.

## 3. Analysis

***Polynomial Solutions.*** Similar to the SMOV calibration (Kozhurina-Platais *et al.*, (2009a, 2009b)), a fourth–order polynomial was used to derive the coefficients of geometric distortion for UVIS and IR, namely:

$$U = A_1 + A_2X + A_3Y + A_4X^2 + A_5XY + A_6Y^2 + A_7X^3 + ... + A_{15}Y^4 \quad (1)$$

$$V = B_1 + B_2X + B_3Y + B_4X^2 + B_5XY + B_6Y^2 + B_7Y^3 + ... + B_{15}Y^4 \quad (2)$$

where $U$ and $V$ are the tangent-plane positions in our astrometric standard catalog, and $X$,$Y$ are the measured pixel positions in the observed UVIS or IR frame. About 40,000 stars were detected in each of the UVIS CCD chip and about 6,000 stars were detected in IR frames from $\omega$ Cen observations – a sufficient number to model properly the geometric distortion with a high-order polynomial. The RMS of these solutions were about 6 *mas* in both UVIS and IR. It is interesting to note, that the RMS of the solution is a factor of three larger than the RMS of 2 *mas* from the Large Magellanic Cloud (LMC) solution, used in SMOV calibration. A simple explanation for such a high RMS is unaccounted intrinsic dispersion of the proper motions of $\omega$ Cen. According to Dinescu *et al.*, (1999), the absolute proper motion of $\omega$ Cen are $\mu_\alpha cos\delta$=–4.9 *mas* and $\mu_\delta$=–3.5 *mas* per year. The epoch difference between WFC3/UVIS & IR observations and the standard catalog is at about 4 years. However, a significant contribution to our solutions is the substantial internal velocity dispersion in proper motion of $\omega$ Cen. As reported by Anderson & van der

Marel (2010) the internal velocity dispersion in the proper motion of $\omega$ Cen is at the level of 0.9 *mas* per year. Approximately, it scales up proportionally with the epoch difference and thus, in four year contributes to the RMS as much as $\sim$4 *mas* or $\sim$0.1 UVIS pixels.

For each of the 10 observed UVIS filters and for each of the 5 observed IR filters, unique polynomial coefficients were obtained which accurately represent the geometric distortion in UVIS and IR filters.

***Multi–Wavelength Distortion.*** The various terms in the general polynomial characterize separate components of the geometric distortion. For example, in the $X$ solution: $A_7$ through $A_{21}$ terms in the general polynomial are classical cubic- and fifth-order distortion terms: the 3rd–order indicate the pin–cushion type of distortion; and the 5th-order terms would indicate the presence of barrel–type of distortion. Specifically to our solution, the 4th-order terms (the terms $A_7$ through $A_{15}$, Eq.1,2) indicate the distortion between pin-cushion and barrel type; while the 2nd order terms, $A_4$ and $A_5$, are the plate tilt terms (van de Kamp, 1967); the linear terms, $A_2$ and $B_3$, are most significant and represent the relative plate scale in $X$ and $Y$. In order to characterize the filter dependency distortion, the linear coefficients $A_2$ and $B_3$ from F606W UVIS solutions (or F160W IR solution) were chosen as a reference scale. Then, the same linear coefficients from the solution in the other filters were transformed into the F606W linear coefficients, namely:

$$X_{scale} = (X_{F606W} - X_{Filter}) \times S \quad (3)$$

$$Y_{scale} = (Y_{F606W} - Y_{Filter}) \times S \quad (4)$$

where $X_{F606W}$ and $Y_{F606W}$ are linear terms $A_2$ and $B_3$ from the UVIS F606W solution (or IR F160W solution) and $X_{Filter}$ and $Y_{Filter}$ are linear terms from the appropriate filter solutions and $S$ is the scale which provides the size of the effect in pixels at the far edge of UVIS detector ($S$=4000 pixels) or IR detector ($S$=1000 pixels).

Figures 1 and 2 show the maximum displacement in UVIS1 and UVIS2 CCD chips due to the scale change *w.r.t.* F606W filter. As seen from these figures, there is a clear correlation in the amount of geometric distortion as a function of wavelength. For example, the difference in the scale in F225W filter is higher by $\sim$0.03% than in F606W. However, the scale difference in in F390W filter is $\sim$0.01% lower than in F606W.

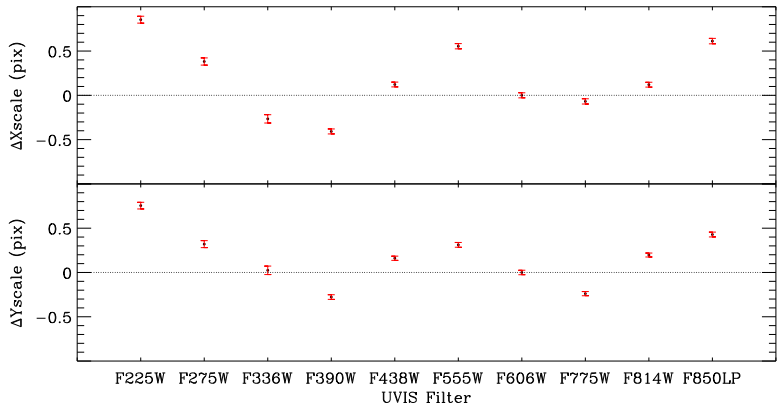


Figure 1: UVIS1 relative scale displacement *w.r.t.* F606W filter. The upper and lower panels show the scale in X and Y for the UVIS1 CCD chip. The scaling by 4000 provides the size of the effect in pixels at the far edge of UVIS detector. The error bars are small compared to the actual scale difference.

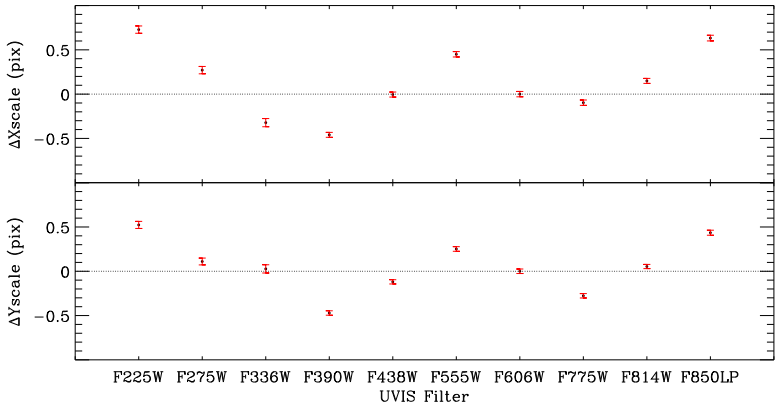


Figure 2: The same as Fig.1 but for UVIS2 CCD chip.

The main reason for the variation in plate scale *vs*. wavelength is variations in the thickness of a filter itself, which is especially significant in the UV filters. Similar filters dependency distortion in WFPC2 filters was reported by Trauger *et al.* (1995), the WFPC2 wavelength-dependent geometric distortion were computed by analyzing the results of ray tracing. The coefficients were presented as quadratic interpolation function of the relative index $n$ of *MgF2* field-flatten lenses. According to Kozhurina-Platais *et al.* (2003), the scale difference in F300W filter is 0.5% higher than in F555W, but in F814W is 0.3% smaller than in F555W.

Figure 3 shows the maximum displacement due to the scale change $w.r.t.$ F160W filter in the IR detector. As seen from Fig.3, the IR scale from filter to filter is quite stable and small (with the exception of F098M). It is a clear indication that the amount of geometric distortion from filter to filter remains nearly constant. Therefore, it is safe to adopt the distortion coefficients from the F160W filter for the other uncalibrated IR filters.

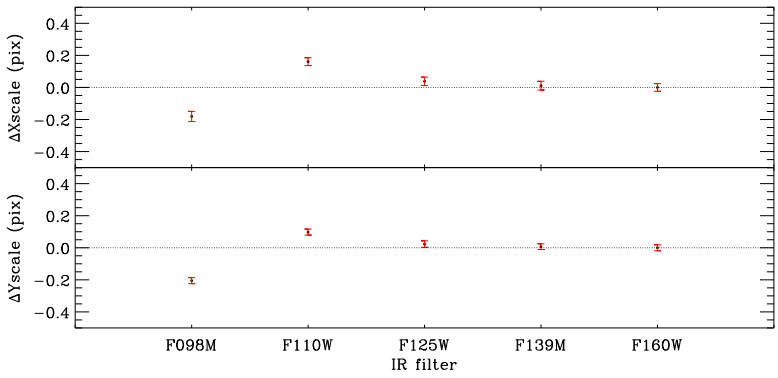


Figure 3: IR filters relative scale displacement $w.r.t.$ F160W filter. Upper and lower panels show the scale in X and Y, respectively. The scaling by 1000 provides the size of the effect in pixels at the edge of IR detector.

***Skew parameter.*** The main parameters, used to quantify the linear part of geometry distortion, are the terms in the general linear transformation between two coordinate systems. As defined in Eq.1 and Eq.2, $U$ and $V$ represent the orthogonal reference coordinate

system, which is free of any systematics in the positions. The $X$, $Y$ coordinate system is the measured frame after applying the distortion correction. Then the linear transformation between these two systems can be expressed as:

$$U = A_1 + A_2X + A_3Y \tag{5}$$
$$V = B_1 + B_2X + B_3Y \tag{6}$$

This 3×2–parameters transformation is a simple linear translation between two coordinates systems (Taff 1980, Kiselev 1989). The rotation angle between these two systems then can be defined as:

$$tan(\theta) = \frac{A_2}{B_3} \tag{7}$$

The skew term, is the amount of non-orthogonality between the two principal X & Y axes and can be derived from the following ratio of linear terms:

$$tan(\gamma) = -\frac{A_2A_3 + B_2B_3}{A_2B_3 - B_2A_3} \tag{8}$$

The skew term is one of the principal geometric distortion parameters, which validates the distortion model. The skew will be constrained accurately in the distortion model if the HST observations are taken with different HST roll–angle, but the skew will not be constrained in the distortion model if the observations are taken with the *same* roll–angle. Also, as it was noticed and discussed by Anderson (2007), the variation of the ACS/WFC linear geometric distortion terms changed monotonically since ACS was installed in 2002.

The skew term, defined above, is the parameter used here for characterization of UVIS geometric distortion. Therefore, we tested the following assumptions:

1. the adopted geometric distortion for the WFC3/UVIS is free of skew;
2. the adopted geometric distortion for the WFC3/UVIS is time–independent.

In order to validate the derived UVIS geometric distortion and possible detect some residual systematics, we used the observations of $\omega$ Cen with different HST roll–angles. The supplemental UVIS calibration program (CAL-12094, PI–L.Petro) was designed so that $\omega$ Cen would be observed through the F606W filter with different roll–angles from –95° to –135° at the step of –10°.

Table 1 lists all observations of $\omega$ Cen with different roll–angles (and *POSTARGS* = 0:0) available to the date (CAL–11452, CAL–11911 & CAL–12094) which were used for characterization of the UVIS geometric distortion.

Table 1: The list of $\omega$ Cen Observations.

| Image ID | Proposal ID | Date-Obs (yy:mm:dd) | WFC3 UVIS Filters | Exp.Time (sec) | Orientat (°) |
|---|---|---|---|---|---|
| iaby02x7q | 11452 | 2009-07-15 | F606W | 35.0 | -28.30 |
| ibc301qrq | 11911 | 2010-01-14 | F606W | 40.0 | 149.76 |
| ibe801nnq | 12094 | 2010-04-25 | F606W | 40.0 | -95.25 |
| ibe802npq | 12094 | 2010-04-25 | F606W | 40.0 | -105.25 |
| ibe803nrq | 12094 | 2010-04-25 | F606W | 40.0 | -135.25 |
| ibe804ntq | 12094 | 2010-04-25 | F606W | 40.0 | -135.25 |
| ibe805nvq | 12094 | 2010-04-25 | F606W | 40.0 | -115.25 |
| ibe806nxq | 12094 | 2010-04-25 | F606W | 40.0 | -95.25 |
| ibe807nzq | 12094 | 2010-04-25 | F606W | 40.0 | -105.25 |
| ibe808o1q | 12094 | 2010-04-25 | F606W | 40.0 | -125.25 |
| ibe809o3q | 12094 | 2010-04-25 | F606W | 40.0 | -125.25 |
| ibc304v3q | 11911 | 2010-04-29 | F606W | 40.0 | -115.25 |
| ibc307qyq | 11911 | 2010-07-04 | F606W | 40.0 | -35.24 |

The so-called $*$`_flt.fits` flat-fielded images, listed above were run through the *Multidrizzle* software (Koekemoer *et al.* 2002) in order to correct for the geometric distortion. Multidrizle software used the new derived multi-filters UVIS geometric distortion coefficients in the form of IDCTAB (Instrument Distortion Correction Table, Hack & Cox (2001)). The X,Y positions from the drizzled images were obtained using the IRAF/DAOPHOT/PHOT task, which includes a Gaussian fit to the PSF and simultaneous aperture photometry. The standard astrometric catalog of $\omega$ Cen as reference frame ($U$,$V$ in Eq. 5–6) and the measured positions ($X$,$Y$ in Eq.5–6) from UVIS drizzled images were used to calculate the skew term (Eq.8) from the linear transformation.

Figure 4 shows the skew as a function of time over one year of the WFC3/UVIS observations. Figure 5 shows skew as a function of time over 3 consecutive HST orbits (short period of time $\sim$ 5 hours). As seen in Fig. 4 the variation of skew appear to be closer to zero, over one year of WFC3 on board. However, Fig.5 with skew over three consecutive HST orbits of observations shows the linear dependency of a skew on the location of HST on orbit.

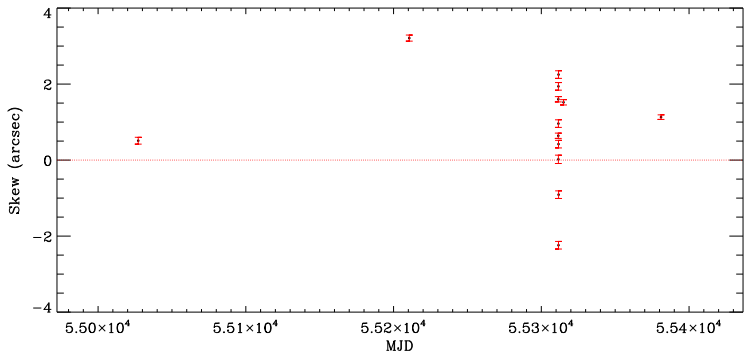


Figure 4: Skew as a function of time spanning over one year for all the WFC3/UVIS observations of globular cluster $\omega$ Cen.

One of the factors in the scale change is the velocity aberration, which across the UVIS detector can vary as much as 5 parts in 100,000 (Cox & Gilliland, 2002). The velocity

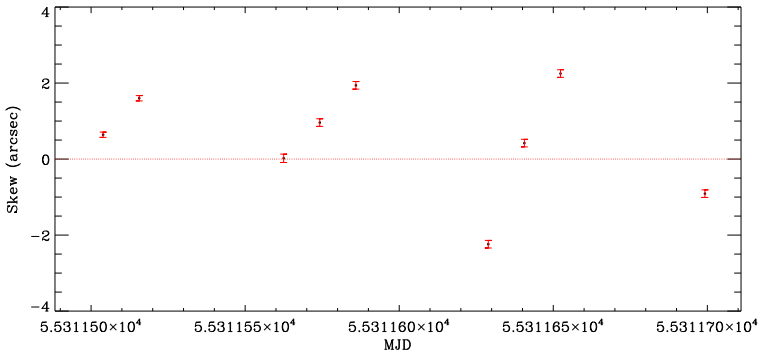


Figure 5: Skew as a function of time from supplemental calibration program (CAL-12094) over 3 consecutive HST orbits.

aberration scale correction factor to the image is available in the header of the science *fits* file and is used by Multidrizzle. Thus, the skew parameter calculated from from drizzled images are velocity aberration free. Another factor in the scale change is the telescope breathing, which takes place on an orbital time scale and causes an effective change of focal length in the optics. Thus, the linear dependency of scale change on a orbital time scale seen in Fig.5 is the so–called thermal breathing. The temporal variations in the scale change due to the thermal breathing from image to image is at the level of ∼0.02%.

As discussed by Anderson (2007), the variation of the skew term for the ACS/WFC has changed monotonically since ACS was installed in 2002. The size of this change is clearly noticeable over 5 years at about 15*mas* off from the original 2002-based distortion solution. This amount of change in distortion is significant for accurate mapping of ACS images with Multidrizzle.

From one year of observations, the WFC3/UVIS geometric distortion is stable within the linear and periodic deviations at about $\pm 3''$ due to the thermal breathing. Scaling by 4000 provides the size of the effect of maximum displacement at the far edge of drizzled images at the level of 0.05 UVIS pixels. From one year of WFC3 UVIS observations, there is no evidence of a *secular* change of the WFC3/UVIS scale.

One of the goals of WFC3 astrometric calibration is to monitor the variation of UVIS and IR distortion over time with a specially designed program so that the standard astrometric field in the vicinity of $\omega$ Cen will be observed several times per year with a nominal HST roll-angle with the steps of $\pm 10°$.

***Lithographic pattern.*** After applying the best–fitting polynomial, the residuals of X & Y positions between the WFC3/UVIS observed $\omega$ Cen frame and the astrometric standard catalog are essentially flat, i.e. all large–scale residuals are successfully removed. Nevertheless, there are a noticeable fine–scale systematic pattern in the residuals from our best–fitting polynomial solutions. Figure 6 shows a 2–D post–solution XY residual map between an observed $\omega$ Cen frame and the astrometric standard catalog. These systematics residuals are typically 0.15 pixels in amplitude and depends on positions of CCD chip.

A complicated and correlated residual structure, placed in fixed–size box seen in Fig.6 is due to the photo–lithography pattern with a size of ∼700×1000 pixels, imprinted onto the detector itself during the manufacturing process. The boundaries of the mask used for photo–lithography are evident. The discontinuities between the vectors coincide with the lithographic boundaries (red lines) as measured in the flat-field images. This very specific complicated structure of residuals shows a typical amplitude of ∼0.1 pixels can not be removed by a polynomial model. It would take a polynomial of higher (up to 15th) order to remove these fine-scale variations. The simple way to remove the fine–scale variations is to

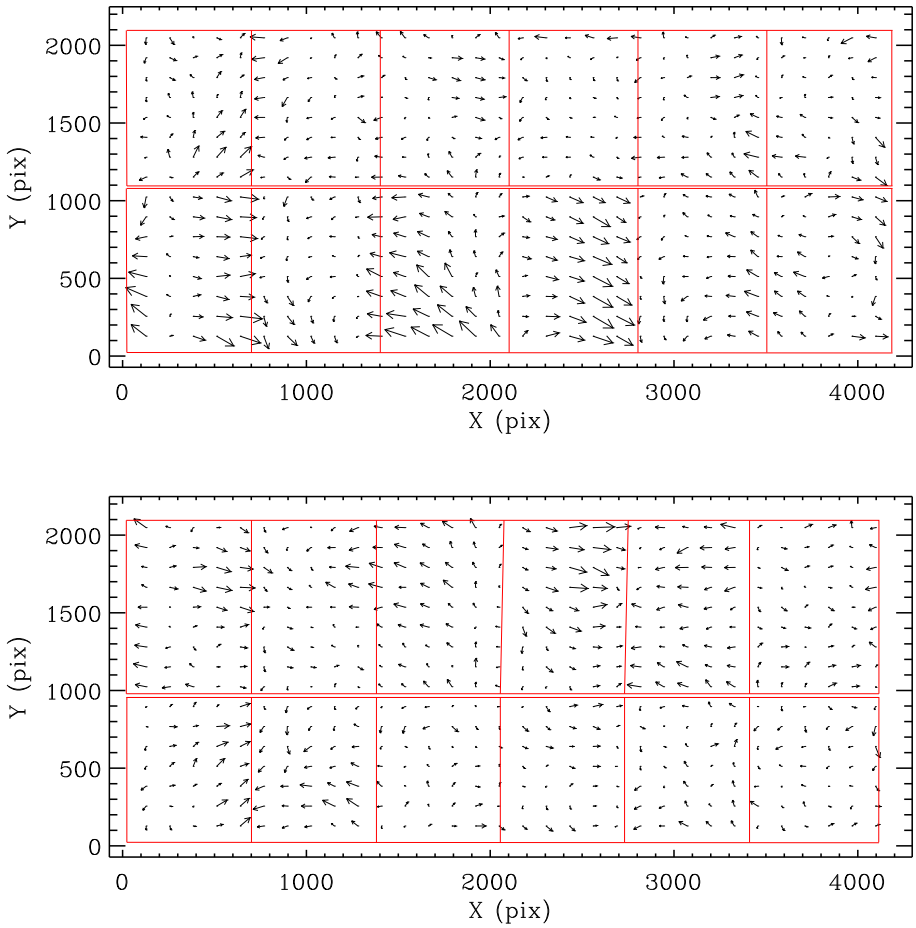


Figure 6: 2–D XY residual map between the UVIS positions corrected for the geometric distortion and the standard astrometric catalog. The top panel shows the XY residuals for the WFC3/UVIS1 CCD chip and the bottom panel shows the XY residuals for WFC3/UVIS2 CCD chip. The boundaries of the photo-lithography mask with size of ∼700×1000 pixels are over–plotted by red boxes. The largest vector is ∼0.15 pixels, magnified by 2500. The unis are WFC3/UVIS pixels.

model the fine–scale structure with look-up table, which can be linearly interpolated at any point in the image. This look-up table would be analogous to ACS/WFC and ACS/HRC (Anderson & King, 2002) as a reference file DGEO in Multidrizzle.

## 4. Conclusion

Here, we presents the results of the WFC3 UVIS and IR multi-wavelength geometric distortion calibration. For each of the 10 observed UVIS filters and for each of the 5 observed IR filters, unique polynomial coefficients were obtained, which accurately represent the geometric distortion in UVIS and IR filters. The derived geometric distortion coefficients in the form of IDCTAB can be successfully used in STSDAS/Multidrizzle software for: 1) stacking of WFC3/UVIS and IR images with different dither pattern; 2) rejecting the CRs; 3) enhance the spatial resolution; 4) deepen the detection limit. The geometric distortion

can be successfully corrected at the 0.1 pixels or 4 and 8 *mas* precision level in UVIS and IR images, respectively.

Summarizing the multi-wavelength geometric distortion for WFC3/UVIS and IR, we conclude that linear scale in the adopted distortion model varies as a function of filters, due to the filters thickness itself. Although, the precision and accuracy of the geometric distortion depends on how accurate and precise is the centering technique for measurement of X and Y positions of under–sample PSF. Because of that, the effective PSF library for each calibrated UVIS filters and PSF fitting technique, developed by Anderson, will allow us to better characterize the WFC3/UVIS multi-wavelength geometric distortion. The next steps in the improvement of UVIS geometric distortion are: 1) implementation of ePSF library and PSF fitting technique for UVIS observations; 2) implementation of the look-up table (DGEO file) in Multidrizzle software to remove the fine–scale variations due to photo-lithography patterns in the WFC3/UVIS images. These two implementations will improve the precision level in the UVIS distorion down to 1 *mas*. However, the precision level in IR distortion mainly depends on how accurate and precise is the centering technique for measurement of X and Y positions of severely under-sample PSF on drizzled IR images.

Summarizing the assessment of the linear part of the WFC3/UVIS geometric distortion, we conclude that for over one year of the WFC3 on HST board, the WFC3/UVIS geometric distortion is time–independent and stable within the linear and periodic deviations at the level of $\pm 0.05$ pixels at the far edge of UVIS drizzled images due to the orbital breathing. We will continue to monitor the variation of the WFC3/UVIS and IR distorion over time.

**Acknowledgments.** We thank Jay Anderson for sharing with his IR *effectivePSF* library and fitting code. V.K-P. especially appreciates the lengthy discussions with Imants Platais and Andrea Bellini for very valuable comments, which improved some asspects of the WFC3 geometric distortion and the text of this paper.

## References

Anderson, J., 2002, in "2002 HST Calibration Workshop", eds. A.Arribas, A. Koekemoer, B.C. Whitmore (Baltimore:STScI), p.18

Anderson, J., 2007, ACS Instrument Science Report, ACS-ISR - 07-08(Baltimore:STScI)

Andesron, J., 2010 (private communications)

Andesron, J., & van der Marel, R.P., 2010, ApJ, 710, 1032-1062

Cox, C., Gilliland, R., 2002, in "2002 HST Calibration Workshop", eds. A.Arribas, A. Koekemoer, B.C. Whitmore (Baltimore:STScI), p.58

Dinescu, D., van Altena, W.,F., Girard, T.M., Lopez, K., 1999, ApJ, 117, 277-285

Hack, W., Cox, C., ACS-ISR - 01-08 (Baltimore:STScI)

Kisilev, A.A., 1989, in "Thereotical Basis of Photographic Astrometry", by Nayka (Moscow, Russia)

Koekemoer, A.,M., Fruchter, A., Hook, R.,N., Hack, W., 2002, in "2002 HST Calibration Workshop", eds A.Arribas, A. Koekemoer, B.C, Whitmore (Baltimore:STScI), p.337

Kozhurina-Platais, V., Anderson, J., Koekemoer, A., 2003, WFPC2 Instrument Science Report, WFPC2-ISR - 03–02 (Baltimore:STScI)

Kozhurina-Platais, V., Cox, C., McLean, B., Petro, L., Dressel, L., Bushouse, H., Sabbi, E., 2009, WFC3 Instrument Science Report, WFC3-ISR - 09–33 (Baltimore:STScI)

Kozhurina-Platais, V., Cox, C., McLean, B., Petro, L., Dressel, L., Bushouse, H., 2009, WFC3 Instrument Science Report, WFC3-ISR - 09–34 (Baltimore:STScI)

Taff, G., L., 1980, in "Computational Spherical Astronomy", John Wiley & Sons, Inc, USA.

Trauger, T.T, Vaughan, A.H., Evans, R.W., Moddy, D.D, 1995, in "Calibrating Hubble Space Telescope: Post Servicing Mission", eds Koratkar, A., Leither, C., (Baltimore:STScI)

van de Kamp, P., 1967, "Principles of Astrometry", by W. H. Freeman & Company (San Francisco and London)